J Mater Sci: Mater Med (2009) 20:2375–2383
DOI 10.1007/s10856-009-3810-5

Preparation and characterization of hydroxyapatite/polycaprolactone–chitosan composites

Xiufeng Xiao · Rongfang Liu · Qiongyu Huang · Xiaohong Ding

Received: 24 March 2009 / Accepted: 24 June 2009 / Published online: 2 July 2009

Abstract Hydroxyapatite (HA)/polycaprolactone (PCL)–chitosan (CS) composites were prepared by melt-blending. For the composites, the amount of HA was varied from 0% to 30% by weight. The morphology, structure and component of the composites were evaluated using environmental scanning electron microscope, X-ray diffraction and Fourier transform infrared spectroscope. The tensile properties were evaluated by tensile test. The bioactivity and degradation property were investigated after immersing in simulated body fluid (SBF) and physiological saline, respectively. The results show that the addition of HA to PCL–CS matrix tends to suppress the crystallization of PCL but improves the hydrophilicity. Adding HA to the composites decreases the tensile strength and elongation at break but increases the tensile modulus. After immersing in SBF for 14 days, the surface of HA/PCL–CS composites are covered by a coating of carbonated hydroxyapatite with low crystallinity, indicating the excellent bioactivity of the composites. Soaking in the physiological saline for 28 days, the molecular weight of PCL decreases while the mass loss of the composites and pH of physiological saline increase to 5.86% and 9.54, respectively, implying a good degradation property of the composites.

1 Introduction

Polycaprolactone (PCL) is a kind of biodegradable aliphatic polyester with good biocompatibility. And it is an ideal scaffold material for its valuable properties such as nontoxicity for organism, gradual resorption after implantation and good mechanical properties [1]. However, in tissue engineering, PCL suffers the disadvantages of (1) poor bioregulatory activity primarily due to its highly hydrophobic nature, (2) slow rate of biodegradation, and (3) susceptibility to microbial action. Due to its low melting point (60°C) and glass transition temperature (−60°C) [2], it could blend with other polymers and allows the modification of its properties to overcome its drawbacks [3–5].

Polymer blends have shown favorable results in terms of the targeted biological, mechanical or degradation properties in comparison to the individual components. Owing to its biocompatibility, biodegradability into nontoxic product, and antimicrobial properties, chitosan has been a much sought after material in a variety of applications including biomedical devices, wound healing, controlled drug delivery and food packing in the past 20 years [6, 7]. Chitosan (CS) ((1 → 4)-2-amino-2-deoxy-β-D-glucan), a mucopolysaccharide, is the alkaline deacetylated product of chitin and has structural similarities to glycosaminoglycans, thus, mimicking their functional behavior. Chitosan is reported to be non-toxic, biodegradable, and biocompatible [8, 9]. The blending of CS and PCL should combine not only good biocompatibility and slow degradation in vivo of both components, but also excellent processibility of PCL [10]. However, the current use of PCL/CS composite in tissue engineering is limited mainly by the lack of bioactivity and the low mechanical property.

Recently, much effort has been made to develop hybrid ceramic/polymer composites, in which bioactive ceramic particles are embedded in a biodegradable polymer matrix. These hybrid composites were found to possess improved mechanical and bioactivity, compared to those of the individual components [11]. Hydroxyapatite (HA, $Ca_{10}(PO_4)_6(OH)_2$) has received a lot of attention for

X. Xiao · R. Liu (✉) · Q. Huang · X. Ding
College of Chemistry and Materials Science, Fujian Normal University, Fuzhou 350007, China
e-mail: rfliu@vip.sina.com

use as a bone graft material, because of its excellent resorbable and osteoconductive properties, which results from its crystallographic and chemical similarity with various calcified tissues in vertebrates [12, 13]. Studies [14–17] on animal testing showed that there was no inflammation around implanted HA, and HA was surrounded by bone tissues and formed an osseous combination with bone tissues. These indicate that HA plays the roles of support and filler of bone and can become a part of the bone skeleton. Therefore, HA has been evaluated as a reinforcing agent with polymers such as high-density polyethylene, poly-L-lactide, polymethyl methacrylate, and polyester-ether to form bioactive compounds [18, 19].

If HA is used as the filler for PCL–CS, the strength of PCL–CS might be improved to meet the clinical requirements. Therefore, the composite based on HA/PCL–CS is a good candidate for preparation of bioabsorbable materials used in various medical fields. Solution blending of HA and polymers have been studied. However, little research has been conducted in the melt blending of polymer and HA. The objective of this research was to evaluate the properties of biodegradable polymer (PCL–CS) reinforced with HA. The amount of HA in the composites was varied from 0% to 30% by weight. The tensile properties (tensile strength and Young's modulus), were evaluated by tensile test. The bioactivity and degradation were investigated after immersing in simulated body fluid (SBF) and physiological saline, respectively. The morphology, structure and component of the composites were characterized.

2 Materials and method

2.1 Materials

HA powder was prepared by hydrothermal method using $Ca(NO_3)_2{\cdot}4H_2O$, and $(NH_4)_3PO_4$ solution as reagents. The pH of $Ca(NO_3)_2$ solution was kept higher than 10.0 and that of $(NH_4)_3PO_4$ solution was kept higher than 11.0 by adding NH_3 solution. A 0.5 M solution of $Ca(NO_3)_2{\cdot}4H_2O$ containing 0.2 g polyethylene glycol was added to $(NH_4)_3PO_4$ solution, and the mixture was stirred for 0.5 h, followed with hydrothermal treatment at 200°C for 8 h. The resultant precipitates were filtered and dried at 100°C overnight.

250 kD, 80-mesh chitosan (~85% deacetylated) powder was purchased from Haidebei Bioengineering Co. Ltd., JiNan, China. PCL was purchased from Daicel chemical Co. Ltd., Japan. All the other chemicals used were of analytical degree.

2.2 Preparation of HA/PCL–CS composites

HA/PCL–CS composites were mixed in the Haake Rheolometer mixer with a blade-type rotor, with rotor speed maintained at 10 rpm and the temperature at 140–150°C. After blending, the composites were pressed into 7 mm-thick plates using a hot press at 140–150°C, then put into a desiccator for cooling. The cooled plates were then made into standard samples for characterization. The blend ratios of HA/PCL–CS composites were 0/95/5, 5/90/5, 10/85/5, 15/80/5, 20/75/5, 25/70/5, 30/65/5 and designated as PCL-HA00–PCL-HA30, respectively.

2.3 Water contact angles test

The hydrophilicity of the composites was evaluated by measuring the water contact angles of the composite disc. Water contact angles were determined using the sessile drop method. The water droplet was 0.5 μl to prevent gravitational distortion of the spherical profile. Each determination was obtained by averaging the results of the three measurements.

2.4 Water absorption

Samples for measuring water absorption were dried in a vacuum oven at 45°C for 24 h, cooled in a desiccator, and then immediately weighed (this weight designated as W_0). Samples were then immersed in distilled water, maintained at 25°C for 24 h test period. Then samples were removed from the water and gently blotted with tissue paper to remove excess water on the surface, and then immediately weighed (designated as W_1). Each W_1 was an average value obtained from three measurements. The percentage increase in weight from water uptake was calculated as follows [20]:

$$\omega = 100 \times (W_1 - W_0)/W_0$$

where, ω is the finial percentage increase in weight of the tested samples.

2.5 In vitro bioactivity

The composite (ω(HA) = 30%) was immersed in a SBF solution with an ion concentration nearly equal to human blood plasma. SBF was prepared as described in the literature [21]. After soaking in SBF for 1 day, 7 days and 14 days, the samples were rinsed with distill water and dried at 40°C.

2.6 In vitro degradation

The in vitro degradation property was evaluated in physiological saline as release medium. Composites were placed into clean beaker with 25 ml physiological saline. The beaker were then sealed and put into an incubator at

constant temperature of 37°C. The samples were removed at intervals of 4 days for the following testing.

The weight losses of composites during degradation were measured by the changes in dry weight after immersion for specified time. For such tests, composites were rinsed in distill water and dried in oven for 24 h. Percent weight loss was calculated according to the following equation [20]:

$$\text{Weight loss}\% = 100 \times (w_0 - w_t)/w_0$$

where, w_0 is the starting dry weight and w_t is the dry weight at specified time.

The pH of the physiological saline at different degradation periods, after samples removal, was measured to monitor change that could be a combination of acidic degradation byproducts resulting from PCL [22] and any neutralization effects resulting from HA and CS.

For molecular weight (M_w) measurement, precisely weighted pieces of the composites were dissolved in chloroform and the inherent viscosity was measured using a Ubbelohde-type viscometer at 30 ± 0.1°C according to the procedure described in [23]. The inherent viscosity [η] was defined by the following equation [24]:

$$[\eta] = \left[2\left(\eta_{sp} - \ln \eta_r\right)\right]^{1/2}/C$$

where, C is the concentration of PCL (0.005 g/ml), η_{sp} and η_r stand for specific viscosity and relative viscosity, respectively. The average molecular weight M_w was then obtained using the Mark–Houwink equation [24]:

$$[\eta] = 1.298 \times 10^{-4} \times M_w^{0.828} \text{ (Chloroform, 30°C)}.$$

2.7 Characterization of the samples

The microstructure of HA powder was investigated using Hitachi600 transmission electron microscope. The crystal structure of prepared composites was investigated by X-ray diffraction (XRD). The prepared composites were cut into slices and then characterized by Philips X'pert MPD diffractometer using Cu Kα generated at 40 kV and 40 mA. The samples were scanned from 10° to 90° with a step size of 0.02° and a count rate of 3.0°/min. Differential scanning calorimetry (DSC) measurements were conducted with Mettle Toledo 822e. To investigate the overall kinetics of isothermal crystallinization, samples were heated from 0°C to 120°C at a rate of 10°C min^{-1}. The melting temperature (T_m) and the melting enthalpy (ΔH) were determined from the heating scan. A Nicolet Avatar 360 spectrometer was used for Fourier transform infrared spectroscopy (FTIR) characterization. Signal averages were obtained for 64 scans at a resolution of 4 cm^{-1}. The samples for FTIR analysis were prepared by grinding the samples with KBr powders and then compressing the mixtures into disks. The morphology of prepared scaffolds was investigated using a Philips XL30 environmental electron microscope (SEM). The stress–strain curves of composites were obtained at 25°C on a LR5KN materials test machine. The tests were performed on "dumbbell" specimens with 7 mm in thickness, length in 30 mm and width in 6 mm at a stretching speed of 10 mm/min. At least five specimens were measured and the mechanical tensile data were determined from the curves on the arithmetic average of three effectively broken specimens.

3 Results and discussion

3.1 Characterization of HA powder

TEM images reveals that the HA particles are rod-shaped with uniform morphology. The particles have an average size of approximately 50–150 nm in length and about 10 nm in width. Representative images of the particles are shown in Fig. 1. It also can be seen that HA particles are distributed not so well with little aggregation.

3.2 XRD analyses

Figure 2 shows the XRD patterns of HA/PCL–CS composite materials with different HA mass fractions. In the first case, two main diffraction peaks, at 2θ around 21.5° and 23.6° attributed to the (110) and (200) planes in PCL

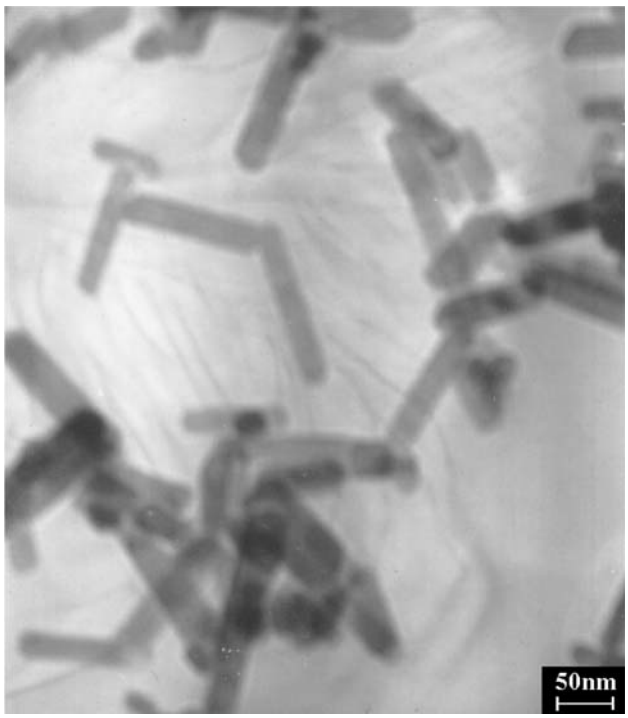

Fig. 1 TEM of HA powders

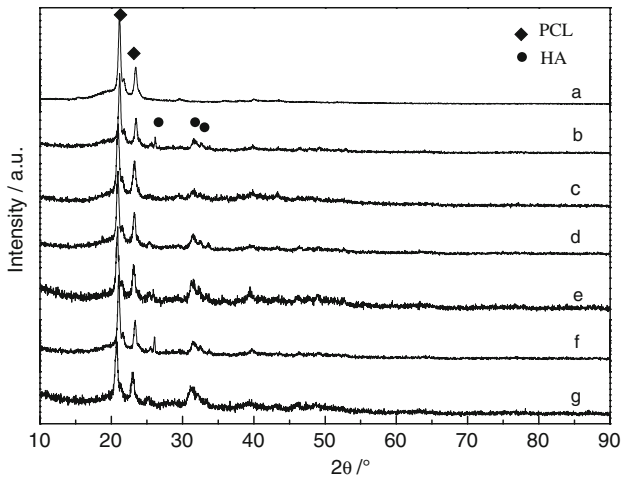

Fig. 2 XRD patterns of HA/PCL–CS composite materials. (a) PCL-HA00; (b) PCL-HA05; (c) PCL-HA10; (d) PCL-HA15; (e) PCL-HA20; (f) PCL-HA25; (g) PCL-HA30

are detected [25], but there is not CS diffraction peaks because of its low crystallinity. The inclusion of HA do not influence the position of the two diffraction peaks of PCL. However, as the HA content in the blend increases, the intensity of the peaks is depressed. The crystallization behavior and crystallinity of PCL are confined by surrounding environment in the hybrids [26]. With the increasing of HA, PCL is embedded in HA microvoid or absorbed on the surface of composites, making PCL crystallize partly. Again, this behavior may be due to the decrease of the content of PCL in the composites.

3.3 DSC analyses

The values of the melting temperature (T_m), melting enthalpy (ΔH) and the degree of crystallinity (X_c) of samples are listed in Table 1. The values of X_c of PCL components are estimated from the ΔH values—assuming that the ΔH value of completely crystalline PCL is 166 J g^{-1} [27]. With increasing HA content in the composite, T_m shifts to higher temperatures and X_c increases in general trend. This could prove that the introduction of HA could affect the crystallinity of PCL in composites and with the increasing of HA content, the crystallinity of PCL increases in some degreed.

Table 1 The thermal properties and crystallinity of PCL

Sample	T_m	ΔH/J g^{-1}	Crystallinity (X_c)/%
PCL-HA00	57.50	59.79	37.91
PCL-HA10	58.50	56.68	40.17
PCL-HA20	59.17	46.66	37.47
PCL-HA30	59.40	44.57	41.31

3.4 Tensile testing

Figure 3 shows the stress–strain curves of the prepared samples. The PCL–CS shows a typical yield point at a strain of ~10%, followed by a steady load with a strain up to ~45% and then a failure. The HA/PCL–CS composites have a similar trend. Compared with PCL–CS, other HA/PCL–CS composites show a relatively brittle failure pattern, with much steeper initial increase in stress with strain up to ~4–14%, followed by an abrupt failure.

Fracture strain, tensile strength and Young's modulus are shown in Fig. 4. The fracture strain decreases with HA content due to HA crystals gradually debonding from the PCL–CS matrix after the neck formation (Fig. 4a). Below the critical composition, the samples undergo the strain-hardening period and the PCL–CS polymer in the samples is regarded as attaining its maximum strain (fracture strain) prior to their fracture. Thus, when the composition surpasses the critical value, the draw stress exceeds the strength of the strain-hardening PCL–CS ligaments in the cross section. Then the samples break at the point where PCL–CS ligaments have not reached the maximum strain. This leads to a sharp decrease of the fracture strain for the case of HA/PCL–CS composite (15%).

Addition of HA leads to a decrease in the tensile strength (Fig. 4b). When the HA content is increased from 5% to 10%, there is a further decrease in tensile strength from 23.00 MPa to 15.43 MPa. The decrease in tensile strength is partially due to the thermodynamic immiscibility and inherent incompatibility between HA and polymer. Yield strength is dependent on the yield strength of the matrix, the decrease of effective load bearing cross section, and the interfacial adhesion between the matrix and the filler and its ability to transfer stresses across the

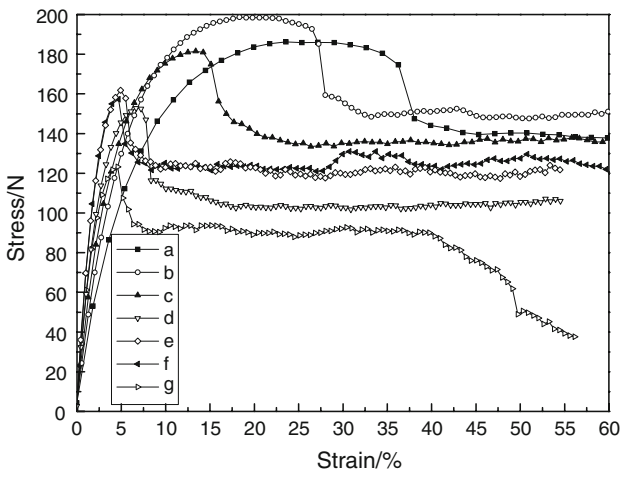

Fig. 3 The stress–strain curves of HA/PCL–CS composite materials. (a) PCL-HA00; (b) PCL-HA05; (c) PCL-HA10; (d) PCL-HA15; (e) PCL-HA20; (f) PCL-HA25; (g) PCL-HA30

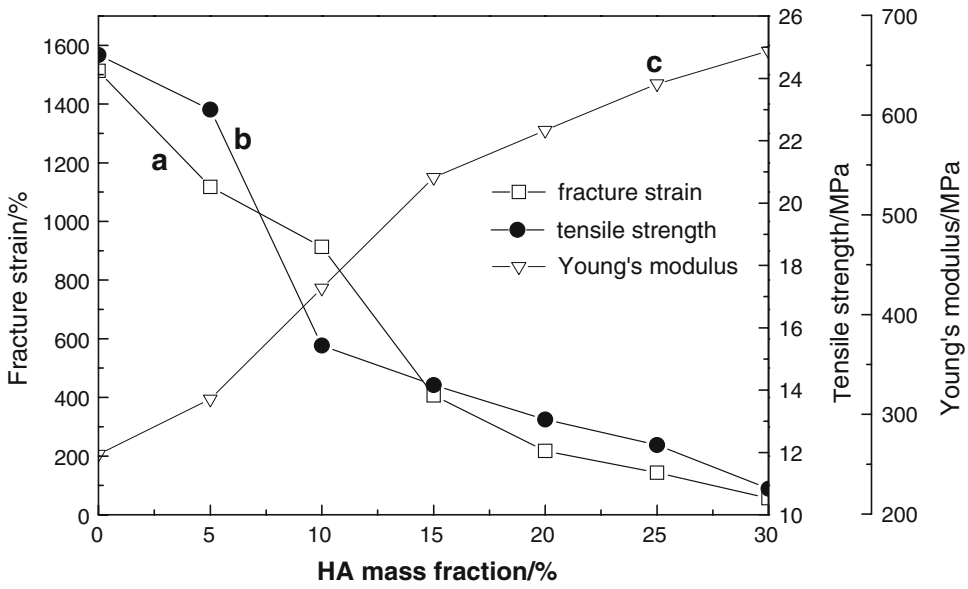

Fig. 4 Relation curves of fracture strain (a), tensile strength (b) and Young's modulus (c) with HA mass fraction

interface [28]. Lack of adhesion led to the formation of pores due to the debonding of the fibers upon the application of stress in a particulate-filled material [29]. As the stress is applied to the blend, lack of interfacial adhesion between HA and polymer will limit the stress transfer process. The lower the HA-matrix adhesion, the lower will be the stress at which debonding occurs, as the fiber are unable to reinforce the composite. In addition, at high HA content, the filler inclusions form aggregates. These aggregates can lead to failure at lower stresses. It can be observed in Fig. 5a–c. The more HA in composite, the more serious aggregate is.

The presence of HA substantially increases the Young's modulus relative to PCL–CS (Fig. 4c). Compared with the PCL–CS, the HA/PCL–CS composites show a much higher Young's modulus, ranging from 316 MPa to 665 MPa. This indicates that the combination of the ductile polymer and hard ceramic filler can mitigate the rubbery or brittle characteristics of the composites derived from the PCL–CS and HA, respectively, thereby allowing the mechanical properties of the composites to be improved.

3.5 Hydrophilicity

Table 2 shows the results of the measurements of water contact angles of the sample's surface. It is obvious that the water contact angles of the samples significantly decrease from 90.96° (PCL/CS) to 62.77° (composite with 30% HA) by the addition of HA, indicating that hydrophilicity increases because of the decreased water contact angle. This result suggests that the incorporation of hydrophilic inorganic materials (HA) into PCL–CS matrix is a feasible approach to improve the hydrophilicity of the polymers. This may be that HA containing lots of hydroxyl group, which could absorb water. From the water uptake, it is found that the water uptake of composites with 0, 10, 20, 30% HA is 1.18%, 2.01%, 2.35% and 3.26%, respectively. It also proves that increasing HA could improve the hydrophilicity of the composites.

3.6 Bioactivity

Bioactivity is thought to be a critical factor in facilitating the chemical fixation of biomaterials to bone tissue, and ultimately the in vivo success of the bone grafting material [30, 31]. Figure 5d–f shows the surface morphology of PCL-HA30 composites after immersing in SBF for 7 days and 14 days. The sporadic mineral growth and pores appear on the surface may be related to the partial dissolution of HA and degradation of PCL and CS during immersion (Fig. 5d). After immersing in SBF for 14 days, there is an obvious coating formed on the surface of the composite, the presence of some cracks are caused due to drying (Fig. 5e). With high magnification, numberless leaves can be observed on the surface of spherical particles (Fig. 5f), the morphology is very similar to that of the deposited apatite on a substrate through biomimetic deposition in SBF.

To identify the coating on the composites, XRD and FTIR were performed and the results are shown in Fig. 6. Figure 6a shows that the diffraction peaks, appearing at 26° and 32° after 14 days immersion become weak, suggesting that formation of apatite with low crystallinity. Figure 6b shows that the peaks at 3,416 cm^{-1} and 1,636 cm^{-1} are the characteristic absorption of H_2O, the absorption bands at 1,034, 602, 564, 465 cm^{-1} are assigned to PO_4^{3-}; the peaks at 874 cm^{-1} and 1,400–1,460 cm^{-1} are the characteristics of CO_3^{2-}, which is an important mark of carbonate

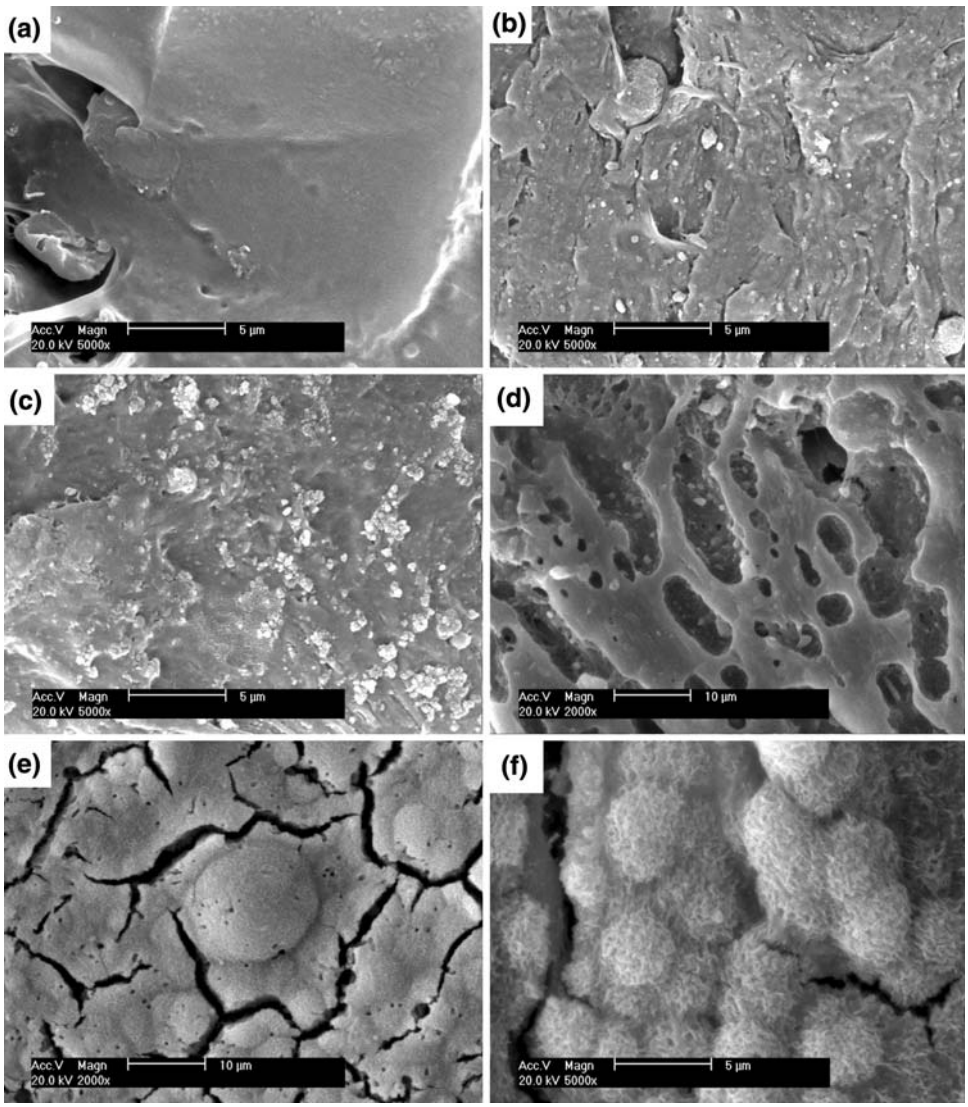

Fig. 5 SEM of the composites **a** PCL–CS, **b** PCL-HA10, **c** PCL-HA30 and the morphologies of the PCL-HA30 composite after immersing in SBF for different time **d** 7 days, **e** 14 days, **f** 14 days, high magnification

Table 2 Water contact angles of the composites

Sample	Water contact angle (°)
PCL-HA00	90.96
PCL-HA10	78.87
PCL-HA20	69.31
PCL-HA30	62.77

group entering into the apatite [32]. So it can be inferred that composites are covered by a coating of carbonated hydroxyapatite (CHA) with low crystallinity, indicating the excellent bioactivity of the composites.

Figure 7 is the pH changes of the SBF used for immersion as a function of immersion time. It shows that pH drops first, then rises and declines afterward. The pH of solution containing composites declines due to the decrease of OH^- at the initial stage. After immersion for 2 h, the pH of the solution is elevated due to the release of alkaline

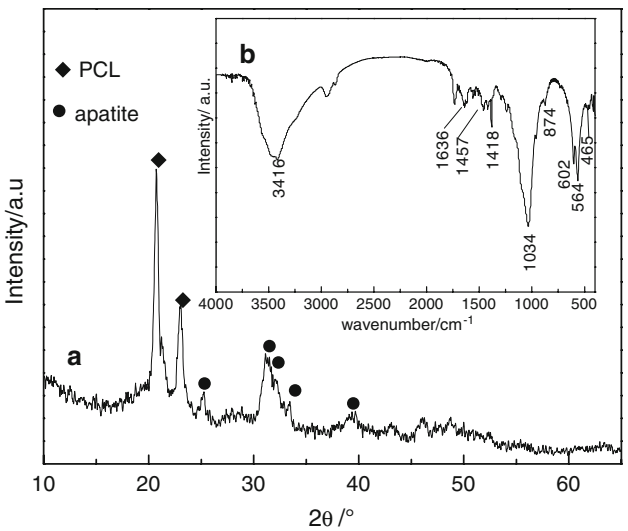

Fig. 6 XRD pattern and FTIR spectrum of the coating on PCL-HA30 composite after immersion in SBF for 14 days

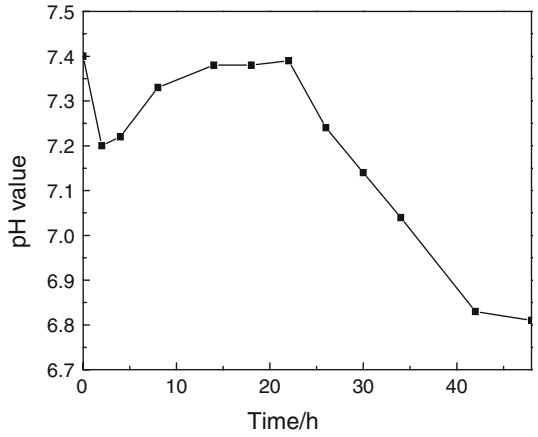

Fig. 7 pH value of the SBF at different time after PCL-HA30 composites immersed in SBF

ions, which are related to the partial dissolution of HA and the degradation of CS. After immersion for 48 h, the pH of the solution declines to 6.81. The filler dissolution rate is important, since the faster the dissolution rate, the faster the ions come into contact with the SBF solution, promoting the surface formation of apatite. Once the apatite crystals are formed, they grow by consuming calcium and phosphate ions from the SBF and carbon dioxide from the atmosphere to form an amorphous carbonated calcium phosphate. As the time prolonged, these amorphous carbonated calcium phosphate transforms into bone-like apatite crystals [33]. The reaction can be expressed as follow:

$$10Ca^{2+} + 6PO_4^{3-} + 2OH^- + 2xCO_3^{2-} + (2-x)\ OH^- \rightarrow Ca_{10}\left[(PO_4)_{6-x}(CO_3)_x\right]\left[(OH)_{2-x}(CO_3)_x\right]$$

After immersion in SBF for 14 days, the mass increment reaches 5.57%, which may be related to the precipitation of CHA.

3.7 In vitro degradation

A biomaterial for bone regeneration applications should firstly bond to the bone and then slowly degrade in such a way that mechanical properties of the implant will adequate to support the regeneration process [34]. Figure 8a shows the changes of molecular weight of PCL with the immersion time prolonged. It indicates that the molecular weight decreases quickly from 7.90×10^4 to 5.11×10^4 in the initial stage, and then decreases slowly. After soaking for 28 days, the molecular weight declines to 3.91×10^4. As seen from Fig. 8b and c the pH and mass loss increase with the immersion time prolonged. After soaking for 28 days, the pH and mass loss reach 9.54 and 5.86%, respectively.

Semicrystalline polyesters–PCL, degrade in two stages. Initially water diffuses into the amorphous regions, resulting in random hydrolytic scission of the ester groups, which may result in additional crystallization. After degradation of the major amorphous regions is initiated, hydrolytic attack shifts towards the center of the crystalline domains [35, 36]. The addition of HA is hypothesized to accelerate the degradation of the PCL polymer. Since HA particles were physically blended into the polymer, they occupied random spaces in the polymer. After immersion in the physiological saline for while, the HA being hydrophilic tends to fall off. The falling of HA creates voids within the polymers, thus exposing their surfaces to

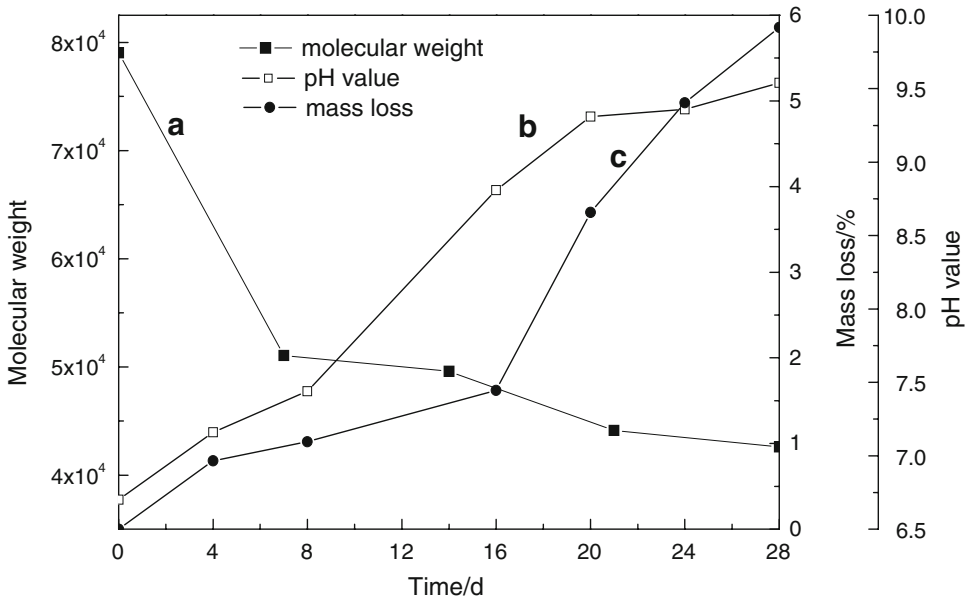

Fig. 8 Relation of molecular weight of PCL (a), pH (b) and mass loss (c) with degradation time

hydrolytic attack and weakening the overall structure of polymers [37]. Molecular weight reduction occurs during immersion in the physiological saline. The hydrophilic fillers–HA, appears to increase the water uptake of the hydrophobic PCL, the molecular weight is reduced to about 3.91×10^4 after 28 days. The pH of the solution containing HA composites is elevated due to the release of alkaline ions, which mainly comes from the partial dissolution of HA and degradation of CS. This behavior could compensate for the pH decrease due to the polymer degradation involving acidic byproducts. Degradation of PCL appears to occur slowly, so that acidic byproducts could not neutralize the alkaline ions in time. Therefore, the pH is increasing all the time, and weight loss is also increasing due to the degradation of PCL, CS and the dissolution of HA.

4 Conclusion

In this paper, HA/PCL–CS composites with different HA ratios were prepared by melt-blending in Haake twin screw extruder. The mechanical property, hydrophilicity, bioactivity and degradation in vitro were investigated. The crystallinity of PCL increases due to the inclusion of HA, and the hydrophilicity improves. The tensile test shows that tensile strength and elongation at break decrease with the increasing of HA, while Young's modulus increases. After immersing in SBF for 14 days, some spherical and weakly crystallized carbonated hydroxyapatite covers on the surface of HA/PCL–CS composites (30% HA), indicating that the composite has excellent in vitro bioactivity. In vitro degradation shows that the molecular weight of PCL decreases from 7.90×10^4 to 3.91×10^4 after immersion in the physiological saline for 28 days, while the mass loss and pH reach 5.86% and 9.54, respectively, indicating a good degradation.

Acknowledgments The authors would like to thanks National Nature Science Foundation of China (30600149), the science research foundation of ministry of Health & United Fujian Provincial Health and Education Project for Tackling the Key Research (WKJ 2008-2-037), the Project of Education Department (209061, JA08030) and Fujian Provincial Department of Science and Technology (No. 2006I0015).

References

1. Tadic D, Bechmann F, Donath T, Epple M. Comparison of different methods for the preparation of porous bone substitution materials and structural investigations by synchrotron (micro)-computer tomography. Materialwissenschaft und Werkstofftechnik. 2004;35:240–4.
2. Sarasam AR, Krishnaswamy RK, Madihally SV. Blending chitosan with polycaprolactone: effects on physicochemical and antibacterial properties. Biomacromolecules. 2006;7:1131–8.
3. Bastioli C, Cerrutti A, Guanella I, Romano GC, Tosin M. Physical state and biodegradation behavior of starch-polycaprolactone systems. J Environ Polym Degrad. 1995;3:81–95.
4. Zhu Y, Gao C, Liu X, Shen J. Surface modification of polycaprolactone membrane via aminolysis and biomacromolecule immobilization for promoting cytocompatibility of human endothelial cells. Biomacromolecules. 2002;6:1312–9.
5. Cascone MG, Barbani N, Cristallini C, Giusti P, Ciardelli G, Lazzer L. Bioartificial polymeric materials based on polysaccharides. J Biomater Sci Polym Ed. 2001;12:267–81.
6. Ng KW, Khor HL, Hutmacher DW. In vitro characterization of natural and synthetic dermal matrices cultured with human dermal fibroblasts. Biomaterials. 2004;25:2807–18.
7. Ouattar B, Simard RE, Piett G, Bégin A, Holley RA. Inhibition of surface spoilage bacteria in processed meats by application of antimicrobial films prepared with chitosan. Int J Food Microbiol. 2000;62:139–48.
8. Chandy T, Sharma C. Chitosan-as a biolmaterial. Biomater Artif Cells Artif Organs. 1990;18:1–24.
9. Goosen MFA. Appplications of chitin and chitosan. Lancaster, PA: Technomic Publishing Co Inc; 1997.
10. Seefried CG Jr, Koleske JV. Lactone polymers VI. Glass-transition temperatures of methyl-substituted ε-caprolactones and polymer blends. J Polym Sci Polym Phys Ed. 1975;13:851–6.
11. Sun JJ, Bae CJ, Koh YH, Kim HE, Kim HW. Fabrication of hydroxyapatite-poly(ε-caprolactone) scaffolds by a combination of the extrusion and bi-axial lamination processes. J Mater Sci: Mater Med. 2007;18:1017–23.
12. Roy DM, Linnehan SK. Hydroxyapatite formed from coral skeletal carbonate by hydrothermal exchange. Nature. 1974;247:220–2.
13. Lavernia C, Schoenung JM. Calcium phosphoate ceramics as bone-substitutes. Am Ceram Soc Bull. 1991;70:95–100.
14. Wang M, Joseph R, Bonfield W. Hydroxyapatite-polyethylene composites for bone substitution: effects of ceramic particle size and morphology. Biomaterials. 1998;19:2357–66.
15. Huang M, Feng JQ, Wang JX. Synthesis and characterization of nano-HA/PA66 composites. J Mater Sci: Mater Med. 2003;14:655–60.
16. Ural E, Kesenci K, Migliaresi M, Piskin E. Poly(D, L-lactide/ε-caprolactone)/hydroxyapatite composites. Biomaterials. 2000;21:2147–54.
17. Zhang SM, Cui FZ, Liao SS, Zhu Y, Han L. Synthesis and biocompatibility of porous nano-hydroxya-patite/collagen/alginate composite. J Mater Sci: Mater Med. 2003;14:641–5.
18. Correlo VM, Boesel LF, Bhattacharya M, Mano JF, Neves NM, Reis RL. Hydroxyapatite reinforced chitosan and polyester blends for biomedical applications. Macromol Mater Eng. 2005;290:1157–65.
19. Wong SC, Bji A. Fracture strength and adhesive strength of hydroxyapatite-filled polycaprolactone. J Mater Sci: Mater Med. 2008;19:929–36.
20. Frank A, Rath SK, Boey F, Venkatraman S. Study of the initial stages of drug release from a degradable matrix of poly (DL-lactide-co-glycolide). Biomaterials. 2004;25:813–21.
21. Tas AC. Synthesis of biomimetic Ca-hydroxyapatite powders at 37°C in synthetic body fluids. Biomaterials. 2000;21:1429–38.
22. Barbanti SH, Zavaglia CAC, Duek EAR. Effect of salt leaching on PCL and PLGA (50/50) resorbable scaffolds. Mater Res. 2008;11:75–80.
23. Pitt CG. Polycaprolactone and its copolymers. In: Chasin M, Langer R, editors. Biodegradable polymer as drug deliver systems. New York: Marcel Dekker Inc; 1990. p. 71–119.
24. Halabalova W, Simek L, Dostal J, Bohdanecky M. Note on the relation between the parameters of the Mark-Houwink-Kuhn-Sakurada equation. Int J Polym Anal Charact. 2004;9:65–75.

25. Chatani Y, Okita H, Tadokoro H, Yamashita Y. Structural studies of polyesters III. Crystal structure of poly-e-caprolactone. Polym J. 1970;1:555–62.
26. Nie KM, Pang WM, Wang YS, Lu F, Zhu QR. Spectral study on intermolecular coupling interaction and relation to microstructure in polyester/inorganic hybrid materials. Spectrosc Spect Anal. 2005;25:537–40.
27. Chen HL, Li LJ, Lin TL. Formation of segregation morphology in crystalline/amorphous polymer blends: molecular weight effect. Macromolecules. 1998;31:2255–64.
28. Pukanszky B, Maurez FHJ, Boode JW. Impact testing of polypropylene blends and composites. Polym Eng Sci. 1995;35:1962–71.
29. Mani R, Bhattacharya M. Properties of injection moulded blends of starch and modified biodegradable polyesters. Eur Polym J. 2001;37:515–26.
30. Davis JE, Baldan N. Scanning electron microscopy of the bone—bioactive implant interface. J Biomed Mater Res. 1997;36:429–40.
31. Marcolongo M, Ducheyne P, Garino J, Schepers E. Bioactive glass fiber/polymeric composites bond to bone tissue. J Biomed Mater Res. 1998;39:161–70.
32. Xiao XF, Liu RF, Gao YJ. Hydrothermal preparation of nanocarbonated hydroxyapatite crystallites. Mater Sci Technol. 2008;24:1199–203.
33. Zhang QY, Chen JY, Feng JM, Cao Y, Deng CL, Zhang XD. Dissolution and mineralization behaviors of HA coatings. Biomaterials. 2003;24:4741–8.
34. Chouzouri G, Xanthos M. In vitro bioactivity and degradation of polycaprolactone composites containing silicate fillers. Acta Biomater. 2007;3:745–56.
35. Mano JF, Sousa RA, Boesel LF, Neves NM, Reis RL. Bioinert, biodegradable and injectable polymeric matrix composites for hard tissue replacement: state of the art and recent developments. Comp Sci Technol. 2004;64:789–817.
36. Proikakis CS, Mamouzelos NJ, Tarantili PA, Andreopoulos AG. Swelling and hydrolytic degradation of poly(D, L-lactic acid) in aqueous solutions. Polym Degrad Stab. 2006;91:614–9.
37. Lei Y, Rai B, Ho KH, Teoh SH. In vitro degradation of novel bioactive polycaprolactone-20% tricalcium phosphate composite scaffolds for bone engineering. Mater Sci Eng C. 2007;27:293–8.